Mineralogical Magazine, October 2017, Vol. 81(5), pp. 1073–1085

Dzierżanowskite, $CaCu_2S_2$ – a new natural thiocuprate from Jabel Harmun, Judean Desert, Palestine Autonomy, Israel

Irina O. Galuskina[1,*], Evgeny V. Galuskin[1], Krystian Prusik[2], Yevgeny Vapnik[3], Rafał Juroszek[1], Lidia Jeżak[4] and Mikhail Murashko[5]

[1] Faculty of Earth Sciences, Department of Geochemistry, Mineralogy and Petrography, University of Silesia, Będzińska 60, 41-200 Sosnowiec, Poland
[2] Institute of Materials Science, University of Silesia, 75 Pułku Piechoty 1A, 41-500 Chorzów, Poland
[3] Department of Geological and Environmental Sciences, Ben-Gurion University of the Negev, POB 653, Beer-Sheva 84105, Israel
[4] Institute of Geochemistry, Mineralogy and Petrology, Warsaw University, al. Żwirki i Wigury 93, 02-089 Warszawa, Poland
[5] Saint Petersburg State University, Faculty of Geology, 7-9 Universitetskaya nab., St. Petersburg, 199034, Russia

[*Received 13 June 2016; Accepted 28 September 2016; Associate Editor: Giancarlo Della Ventura*]

ABSTRACT

Dzierżanowskite, $CaCu_2S_2$ ($P\bar{3}m1$, $a = 3.9400(4)$, $c = 6.523(1)$ Å, $V = 87.69(2)$ Å^3, $Z = 1$), a thiocuprate, was found in larnite pseudoconglomerate rocks of the Hatrurim Complex at Jabel Harmun, Palestinian Autonomy, Israel. Dzierżanowskite occurs in larnite pebbles, which are embedded in a low-temperature mineral matrix. Associated minerals are larnite, brownmillerite, fluorellestadite, ye'elimite, gehlenite, periclase, ternesite, nabimusaite, vorlanite, vapnikite, fluormayenite, fluorkyuygenite, oldhamite, jasmundite, covellite, chalcocite and pyrrhotite. Electron microprobe analyses yield an average composition of Cu 55.25, Fe 0.13, S 27.46 and Ca 16.99, total 99.83 wt.%. The empirical formula of dzierżanowskite, based on 5 atoms, is $Ca_{0.98}Cu_{2.02}Fe_{0.01}S_{1.99}$. Dzierżanowskite forms grains up to 15 μm in size or rims on oldhamite and laminar intergrowths with chalcocite and covellite. Dzierżanowskite is dark orange, has a cream streak and a submetallic lustre. In reflected light it is grey, with a cream tint and characteristic yellow-orange internal reflections. The calculated density of dzierżanowskite is 4.391 g cm^{-3}. Three bands at 300, 103 and 86 cm^{-1} are observed in the Raman spectrum. The strongest lines of the calculated powder diffraction pattern are [*d*, Å (*I*) *hkl*]: 2.358(100) 102, 1.970(93)110, 3.023(78) 011, 6.523(36) 001, 3.412 (28) 100, 1.834(28) 103. Dzierżanowskite was also found in unusual jasmundite rocks, forming small 'paleofumaroles' within areas of low-temperature hydrothermal rocks bearing larnite pseudoconglomerates at Jabel Harmun. Dzierżanowskite is a superimposed phase of the high-temperature alteration of pyrometamorphic rocks subjected to by-products (melts/fluids and gases) of pyrometamorphism originating in the deeper levels of combustion.

Keywords: dzierżanowskite, $CaCu_2S_2$, new mineral, thiocuprate, Jabel Harmun, Hatrurim Complex.

Introduction

Dzierżanowskite (IMA2014-032), $CaCu_2S_2$ ($P\bar{3}m1$, $a = 3.9400(4)$, $c = 6.523(1)$ Å, $V = 87.69(2)$ Å^3, $Z = 1$) was found in pyrometamorphic (combustion metamorphic) rocks of the Hatrurim Complex ("Mottled Zone"; Bentor, 1960; Gross, 1977; Vapnik *et al.*, 2007; Sokol *et al.*, 2007, 2010; Novikov *et al.*, 2013) on Jabel Harmun (Jabel = mountain in Arabic). The type locality, near the Palestinian village of Nabi Musa, lies close to a historical place with an eponymous name (probably the Tomb of Moses), situated in the Judean Desert, West Bank, Palestinian Autonomy, Israel (31°46′N, 35°26′E).

Dzierżanowskite, $CaCu_2S_2$, belongs to the thiocuprate group of minerals (Boller, 2007); its

*E-mail: irina.galuskina@us.edu.pl
https://doi.org/10.1180/minmag.2016.080.153

synthetic analogue (Purdy, 1998), related to the structural type $CaAl_2Si_2$, is known (Condron *et al.*, 2007). Chvilevaite $Na(Cu,Fe,Zn)_2S_2$, is the only mineral of note among the natural phases (Kachalovskaya *et al.*, 1988), characterised by a structure similar to dzierżanowskite. The chvilevaite structure with disordered distribution of Cu with mixed valence, Fe^{2+} and Zn in tetrahedral sites, was refined in the non-centrosymmetric *P*3*m*1 space group ($a = 3.873$ Å, $c = 6.848$ Å, $V = 88.959$ Å^3; Kaplunnik *et al.*, 1990) as differing from $CaCu_2S_2$ (Purdy, 1998). Natural $CaCu_2S_2$ was detected in 2012 by Piotr Dzierżanowski during a study of the composition of sulfides in larnite rocks in probe no. MII-33 (M. Murashko's collection) on a CAMECA SX100 microprobe analyser. Three new minerals, vapnikite, Ca_3UO_6 (Galuskin *et al.*, 2014), nabimusaite, $KCa_{12}(SiO_4)_4(SO_4)_2O_2F$ (Galuskin *et al.*, 2015*a*) and its Ba-analogue dargaite, $BaCa_{12}(SiO_4)_4(SO_4)_2O_3$, were discovered in the same probe sample. Dargaite as new species has been studied from Nahal Darga, Judean Desert, Palestinian Autonomy (Gfeller *et al.*, 2015*a*).

The name is given in honour of Dr Piotr Dzierżanowski (1947–2015) from the Institute of Geochemistry, Mineralogy and Petrology, University of Warsaw, Poland. Piotr Dzierżanowski was a recognized expert in microprobe analyses and was connected intimately with the development of Polish mineralogy during the last 15 years. His premature death is a major loss for Polish science; he was a co-author of the descriptions of 31 new mineral species from the pyrometamorphic and metasomatic rocks of Israel and the Caucasus and Baikal regions, Russia.

Until recently, specimen no. MII-33 was the only sample in which dzierżanowskite, approved by CNMNC IMA in 2014, was found. A fragment of the holotype, specimen no. MII-33 is deposited in the collections of the Mineralogical Museum, University of Wrocław, Cybulskiego 30, 50-205 Wrocław, Poland, catalogue number MMUWr II-20464.

In 2015 we found unusual jasmundite, apoflamite rocks at Jabel Harmun, in which dzierżanowskite is well represented. Jabel Harmun is the type locality (the outcrop of pyrometamorphic rocks of the Hatrurim Complex is a few km^2 in area) of several new minerals: harmunite $CaFe_2O_4$ (IMA2012-045, Galuskina *et al.*, 2014), nabimusaite $KCa_{12}(SiO_4)_4(SO_4)_2O_2F$ (IMA2012-057, Galuskin *et al.*, 2015*a*), fluormayenite $Ca_{12}Al_{14}O_{32}F_2$ (IMA2013-019, Galuskin *et al.*, 2015*b*), vapnikite Ca_3UO_6 (IMA2013-082, Galuskin *et al.*, 2014); and gazeevite, $BaCa_6(SiO_4)_2(SO_4)_2O$ (IMA2015-37, Galuskin *et al.*, 2017). In the present paper we characterize dzierżanowskite from the holotype specimen no. MII-33, representing the larnite rock, and from recently found jasmundite-rich rocks. We also discuss the mechanism and conditions of dzierżanowskite formation.

Methods

The crystal morphology and composition of dzierżanowskite and associated minerals were examined using optical microscopy, a scanning electron microscope (Philips XL30 ESEM/EDAX, Phenom XL; Faculty of Earth Sciences, University of Silesia), and electron microprobes CAMECA SX100 and CAMECA SXFiveFE (Institute of Geochemistry, Mineralogy and Petrology, University of Warsaw). Chemical analyses were carried out on the electron microprobe (15 kV, 20 nA, 1–2 μm beam diameter) using the following lines and standard materials: As*L*α – GaAs, Zn*K*α – sphalerite; Cu*K*α, Fe*K*α, S*K*α – $CuFeS_2$; Pb*M*α – PbS; Ni*K*α – NiO; Co*K*α – CoO; Ag*L*α – Ag_2Te; Ca*K*α – diopside, Se*L*α – Bi_2Se.

The Raman spectrum of dzierżanowskite was recorded on a WITec alpha 300 confocal Raman microscope (Jagiellonian Centre for Experimental Therapeutics, Krakow, Poland) equipped with an air-cooled solid state laser (488 nm) and a CCD camera (–62°C). Raman-scattered light was fed into a microscope through a 50 μm diameter optical fibre and monochromator with a 600 mm^{-1} grating. An air Olympus MPLAN (100x/0.90NA) objective was used. The power of the laser at the sample position was 12 mW. Some 15–20 scans with integration times of 10–15 s and resolution 3 cm^{-1} were collected and averaged. The monochromators of both spectrometers were calibrated using the Raman scattering line of a silicon plate (520.7 cm^{-1}).

Dzierżanowskite forms inhomogeneous, separate grains 10–15 μm in size and intergrowths with other sulfides. It is commonly partially oxidized, which effectively excludes the possibility of extracting a single crystal. Thus, the symmetry and cell parameters of dzierżanowskite were determined by electron back-scatter diffraction (EBSD) using a JEOL JSM-6480 scanning electron microscope (SEM) equipped with EBSD (University of Silesia, Poland). The EBSD images were recorded with a HKL Nordlys II camera using 30 kV beam energy. The EBSD study was performed on microprobe thin sections repolished with an Al_2O_3 suspension of

20 nm particle size. Calibration of the geometry of the SEM and EBSD system was carried out on Si for two detector distances, i.e., 177 mm (normal working position) and 150 mm (camera refracted position). The program *Channel5* (Day and Trimby, 2004) was used for the interpretation of the EBSD diffraction patterns.

Occurrence and description

The holotype specimen no. MII-33 is a fragment of a dark-brown larnite pebble from a pseudoconglomerate of the Hatrurim Complex, collected by M. Murashko in 2008 on the south slope of Jabel Harmun, Judean Desert, Palestinian Autonomy, Israel. Rocks of the Hatrurim Complex are distributed widely in the region surrounding the Dead Sea in the territory of Israel, Palestinian Autonomy and Jordan (Picard, 1931; Kolodny and Gross, 1974; Burg *et al.*, 1991, 1999). The larnite rocks were formed during pyrogenic metamorphism due to caustobiolith combustion at temperatures above 800°C (Kolodny and Gross, 1974; Sokol *et al.*, 2007, 2010). Their pebble-like shape can be explained by low-temperature hydrothermal alteration of larnite-rich rocks with subsequent weathering (Gross, 1977). A geological description of the Jabel Harmun locality and existing hypotheses for the genesis of pyrometamorphic rocks of the Hatrurim Complex are summarized by Galuskina *et al.* (2014 and references therein).

The holotype specimen of dzierżanowskite (no. MII-33) is a larnite-ye'elimite-fluorellestadite-brownmillerite rock with an inhomogeneous distribution of minerals of the fluormayenite–fluorkyuygenite series. This rock is partitioned by a network of light, bluish veins characterized by higher porosity, in which larger grains of larnite, fluorellestadite, brownmillerite and ye'elimite, and newly-formed ternesite, nabimusaite, jasmundite and Ca, Cu, Fe, Ni, Ag sulfides are noted (Fig. 1*a*, see also fig. 3 in Galuskin *et al.*, 2015*a*). Accessory minerals in the dark part of the rock are vapnikite, vorlanite, periclase, shulamitite, magnesioferrite-spinel, gehlenite, pyrrhotite and baryte. Grains of dzierżanowskite, up to 15 μm in size, occurs in association with Cu sulfides, represented by chalcocite, covellite, anilite, djurleite and oldhamite (Figs 1, 2; Table 1). Dzierżanowskite forms rims on oldhamite and laminar intergrowths with chalcocite and covellite (Fig. 1*b*, *c*). Micrometre-sized sulfides of Ni, Zn, Pt, Pd, Ag and selenides of Cu and Ag form inclusions in chalcocite; according to results from SEM energy-dispersive spectroscopy, heazlewoodite, polydymite, vysotskite, naumannite, braggite, millerite and sphalerite were determined. Submicrometre-sized grains of $CaNi_2S_2$, $BaCu_2S_2$, KCu_4S_3 and a murunskite-like phase, $K_2Cu_3FeS_4$, are also found in association with dzierżanowskite. Dzierżanowskite is characterized by a dark orange colour, a cream streak and submetallic lustre. In reflected light it is grey, with a cream tint and characteristic yellow-orange internal reflections (Fig. 2*b*). The density could not be measured because of the small grain size; the calculated density is 4.391 g cm^{-3} using the empirical formula $Ca_{0.98}Cu_{2.02}Fe_{0.01}S_{1.99}$ (Table 1, analysis 1). Dzierżanowskite shows strong orange cathodoluminescence; partially hydrated dzierżanowskite grains have weak yellowish cathodoluminescence.

In 2015, the second discovery of dzierżanowskite was connected with the finding of unusual jasmundite (apo-flamite) rocks, forming, as a rule, rounded bodies (forms), so-called 'paleofumaroles', 1–1.5 m across in low-temperature hydrothermal rocks bearing larnite pseudoconglomerates (Fig. 3*a*). There are four such 'fumaroles' on the south-west slope of Jabel Harmun. Jasmundite forms chains of crystals along cracks in these rocks (Fig. 3*b*) and spot-like aggregates of xenomorphic grains (Fig. 4*a*), the size of which is much bigger than the size of the mineral grains in the primary pyrometamorphic association. The primary pyrometamorphic association is represented by flamite-brownmillerite rocks (Fig. 3*c*). Flamite is partially hydrated and contains inclusions of nabimusaite, ternesite and fluorellestadite (Fig. 3*c*, 4*a*; see also fig. 8 of Galuskin *et al.*, 2016). Eutectic intergrowths of fluormayenite and flamite, on the rims of which thin zones of brownmillerite have crystallized (Fig. 4*a*, *b*), are a characteristic feature of flamite rocks. Fluormayenite is almost completely replaced by fluorkyuygenite.

Studies of unaltered fractures in the rocks showed that oval inclusions of flamite with dissolved surfaces and abundant micrometre-sized Cu-sulfides are widespread in the jasmundite (Fig. 3*d*). Sometimes, rounded empty channels with smooth, unaltered walls are noted in the jasmundite. More often these channels are filled with calcite, ettringite or Cl-bearing Ca-hydrosilicates. In such cases the jasmundite forming the walls of the channels is intensively hydrated (Fig. 3*d*). In specimen no. JBB4 dzierżanowskite

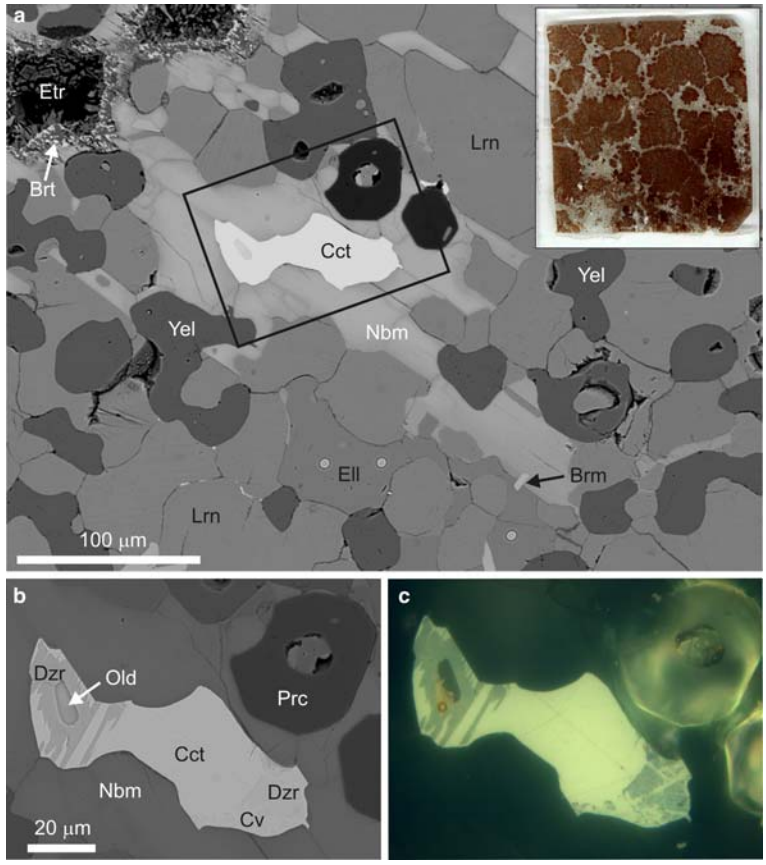

FIG. 1. (*a*) Back-scattered electron (BSE) image of a chalcocite grain with oldhamite inclusions in altered larnite rock (holotype specimen MII-33), Jabel Harmun, Palestinian Autonomy; the black frame marks the area magnified in Fig. 1*b* and *c*; an image of the thin section in normal light is inset top right (field of view = 2 cm). (*b*) BSE image of dzierżanowskite overgrowing an oldhamite inclusion on the contact with chalcocite. (*c*) Reflected light image of (*b*); dzierżanowskite is grey; the brown circle is a crater formed after measurement in a Raman microscope at high power of laser. Dzr = dzierżanowskite, Cct = chalcocite, Cv = covellite, Lrn = larnite, Ell = fluorellestadite, Brm = brownmillerite, Nbm = nabimusaite, Yel = ye'elimite, Brt = baryte, Etr = ettringite, Prc = periclase.

usually forms thin rims on rounded oldhamite grains, sometimes almost completely replacing it (Fig. 4*c*, *d*). Rarer oldhamite and dzierżanowskite build complex mineral aggregates together with newly-formed brownmillerite, fluorellestadite and Cu-sulfides (Fig. 4*e*). Between dzierżanowskite and jasmundite small zones of chalcocite or covellite occur, where sulfides form subtle worm-like inclusions in jasmundite (Fig. 4*d*). Other Ca, Cu, Fe, Ni, Ag sulfides and, rarely, exotic K and Na sulfides, for example the Na-analogue of murunskite (Fig. 4*d*; Table 1, analysis 9), are found in specimen no. JBB4 together with jasmundite as well as in the holotype specimen.

EBSD and Raman data for dzierżanowskite

Single-crystal X-ray studies could not be performed because of the small crystal size. Structural data were obtained using EBSD techniques (Fig. 5) and by fitting data to the structural model of synthetic $CaCu_2S_2$ (Purdy, 1998). The preparation of the dzierżanowskite surface for EBSD study was critical because of the limited amount of the holotype specimen no. MII-33, so the quality of the Kikuchi images obtained for dzierżanowskite and the associated oldhamite was rather low (Fig. 5). The EBSD pattern for dzierżanowskite was obtained at working distances 155 and 177 mm. Fitting of the

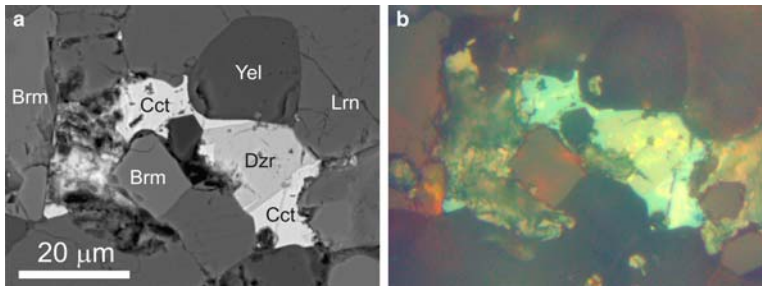

FIG. 2. One of the largest segregations of dzierżanowskite in holotype specimen MII-33: (*a*) BSE image. (*b*) Reflected light, poor polishing of chalcocite has resulted in its blue hue (covellite); dzierżanowskite is grey with cream hue, light-orange internal reflexes are visible in it; brownmillerite shows red internal reflexes. Dzr = dzierżanowskite, Cct = chalcocite, Lrn = larnite, Brm = brownmillerite, Yel = ye'elimite.

EBSD pattern at 177 mm for a $CaCu_2S_2$ model with $a = 3.9400(4)$, $c = 6.523(1)$ Å, $V = 87.69(2)$ Å^3, $Z = 1$, space group: $P\bar{3}m1$ (Purdy, 1998) resulted in the parameter MAD = 0.46° (good fit). More qualitative Kikuchi images for the working distance 177 mm were obtained for dzierżanowskite and oldhamite from specimen no. JJB4 (Fig. 4*e*; Fig. 6*a*,*b*). We also tried to determine the Cu-sulfides intergrowing with dzierżanowskite and oldhamite using the EBSD method. Cu-sulfides with stoichiometry close to

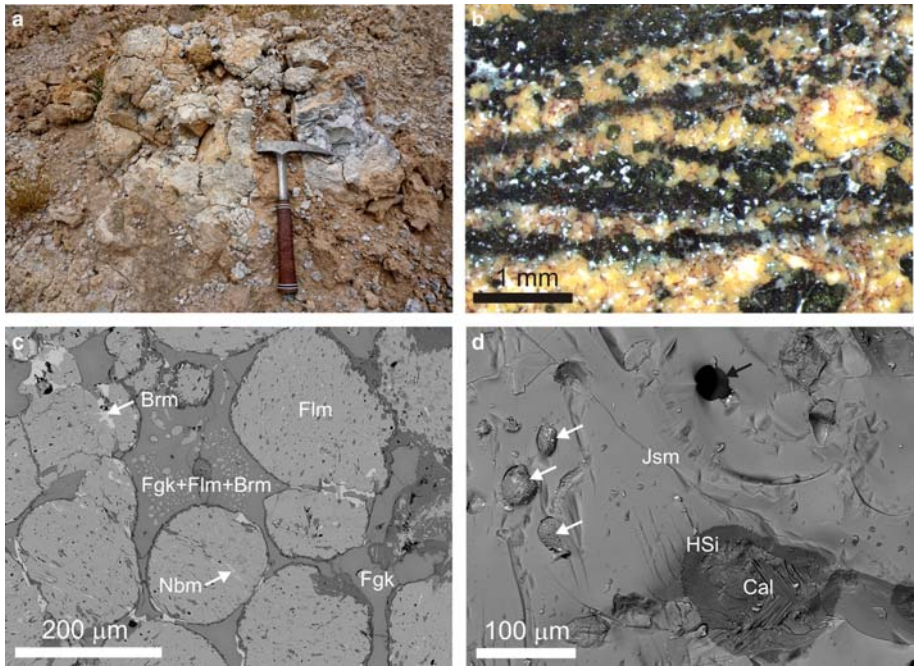

FIG. 3. (*a*) Jasmundite rock outcrop on the south slope of the Jabel Harmun, where dzierżanowskite was found. (*b*) Dark-green jasmundite crystals form chain-like aggregates along fissures in altered flamite rock; brownmillerite rims (red) are visible on flamite grains (yellow). (*c*) Altered flamite rock: BSE image of a yellow fragment of the rock. (*d*) Fresh fracture of a jasmundite crystal; oval inclusions of flamite relics are shown by white arrows; and a hollow channel is shown by a black arrow. A channel with hydrated walls filled by calcite is visible at bottom right corner. Dzr = dzierżanowskite, Flm = flamite, Brm = brownmillerite, Nbm = nabimusaite, Fkg = fluorkyuygenite, Cal = calcite, Jsm = jasmundite, HSi = hydrosilicate.

TABLE 1 Representative compositions of dzierżanowskite and associated sulfide minerals.

	MII- 33			JBB4	MII-33						JBB4	
Anal. no.*	[1]			[2]	[3]	[4]	[5]	[6]	[7]	[8]	[9]	[10]
wt.%	Mean $n=9$	s.d.	range	mean $n=3$								
Ag	n.d.			n.d.	n.d.	1.80	n.d.	1.00	n.d.	25.47	n.d.	n.d.
Zn	n.d.			n.d.	n.d.	n.d.	n.d.	n.d.	0.19	n.d.	n.d.	n.d.
Cu	55.25	0.55	54.26–55.93	55.78	34.69	77.62	79.79	78.42	65.16	52.67	48.26	n.d.
Fe	0.13	0.10	0–0.30	0.13	30.37	0.00	0.12	0.00	0.00	0.00	12.04	n.d.
S	27.46	0.17	27.24–27.64	27.81	35.28	19.67	23.01	20.58	32.50	14.04	30.18	43.78
Se	n.d.			n.d.		0.26	n.d.	0.27	0.47	7.97	n.d.	n.d.
Ca	16.99	0.21	16.73–17.37	16.52	0.00	0.20	0.25	0.23	0.60	0.33	0.43	55.36
Na	n.d.			n.d.	n.d.	n.d.	n.d.	n.d.	n.d.	n.d.	9.71	n.d.
Total	99.83			100.24	100.34	99.55	103.17	100.50	98.92	100.48	100.62	99.14
	Calculated on atoms per formula unit											
	5			5	4	3	10	47	2	3	10	2
Ca	0.98			0.95		0.01	0.03	0.14	0.01	0.02	0.05	1.01
Na											1.80	
Cu	2.02			2.03	1.00	1.97	6.97	30.62	0.99	1.54	3.23	
Ag						0.03		0.23		0.44		
Fe	0.01			0.01	0.99		0.01				0.92	
S	1.99			2.01	2.01	0.99	3.98	15.93	0.98	0.81	4.01	0.99
Se						0.01		0.09	0.02	0.19		

*Key: [1], [2] – dzierżanowskite, ~ $CaCu_2S_2$; [3] – chalcopyrite, ~ $CuFeS_2$; [4] – chalcocite; ~ Cu_2S; [5] – anilite, ~ Cu_7S_4; [6] – djurleite, ~ $Cu_{31}S_{16}$; [7] – covellite, CuS, [8] – covellite-like mineral, ~ $(Cu,Ag)_2(S,Se)_1$; [9] – Na-analogue of murunskite, ~ $Na_2Cu_3FeS_4$; [10] – oldhamite, ~ CaS.

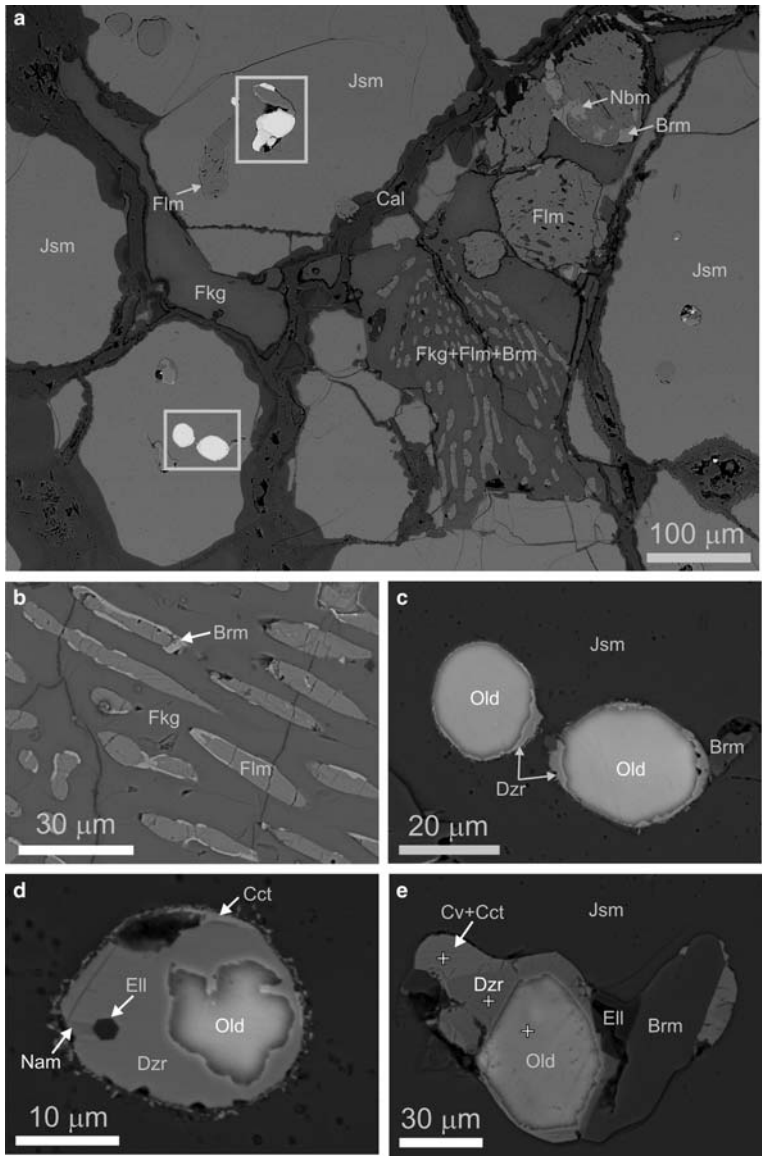

FIG. 4. (*a*) Typical view of altered flamite rock, in which oval inclusions of oldhamite and Cu-sulfides are hosted, mainly, in large jasmundite grains. Eutectic intergrowths of flamite and fluorkyuygenite (primary, fluormayenite), fragments in the frame are magnified in Fig. 4*e*. (*b*) brownmillerite crystallized in eutectic intergrowths on the boundary of flamite and fluormayenite. (*c*) Thin rims of dzierżanowskite on oldhamite. (*d*) Oval segregation of dzierżanowskite with oldhamite relics, chalcocite external thin rim, fluorellestadite and the Na-analogue of murunskite inclusions. (*e*) Oldhamite inclusion in jasmundite with dzierżanowskite rims intergrowing with chalcocite–covellite and brownmillerite. Kikuchi (EBSD) images were obtained at points marked by crosses. Dzr = dzierżanowskite, Cct = chalcocite, Cv = covellite, Lrn = larnite, Flm = flamite, Ell = fluorellestadite, Jsm = jasmundite, Fkg = fluorkyuygenite, Brm = brownmillerite, Nbm = nabimusaite, Cal = calcite, Nam = Na-analogue of murunskite.

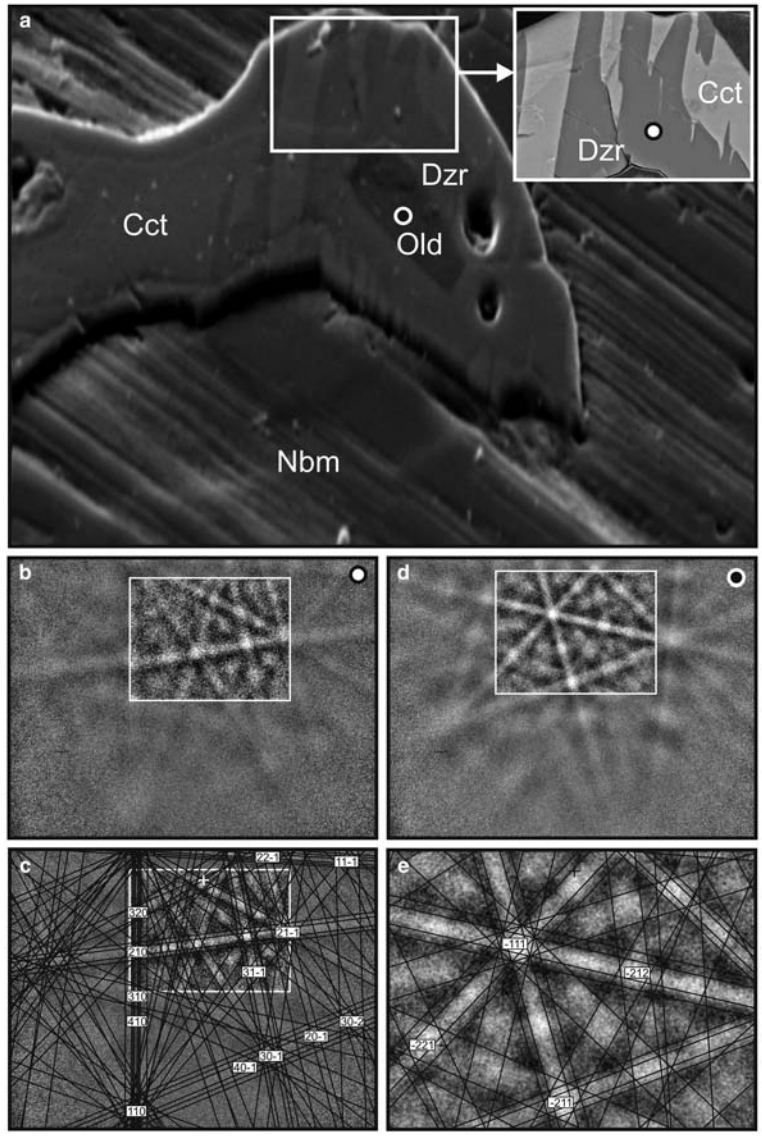

FIG 5. EBSD patterns of dzierżanowskite and oldhamite. (*a*) High relief image of minerals in thin-section (Fig. 1) after colloidal silica treatment; a fragment limited by the frame is shown in the inset as a BSE image (circles show points at which EBSD patterns of dzierżanowskite and oldhamite were obtained). (*b*) EBSD patterns of dzierżanowskite for working distances of 177 mm and 155 mm (shown in frame). (*c*) Fitted result of the EBSD pattern with the $CaCu_2S_2$ model for a working distance of 177 mm, MAD = 0.46° (good). (*d*) EBSD patterns of oldhamite for working distances of 177 mm and 155 mm (in frame). (*e*) Fitted result of the EBSD pattern for a working distance of 155 mm, MAD = 0.72°. Dzr = dzierżanowskite, Cct = chalcocite, Old = oldhamite, Nbm = nabimusaite.

chalcocite after preparation of the surface using colloidal Al_2O_3 usually did not provide a Kikuchi image or showed a fuzzy Kikichi image, fitting of which pointed to covellite (Fig. 6*c*).

Because micrometre-sized dzierżanowskite occurs only in small concentrations, powder X-ray diffraction data could not be collected. Powder X-ray diffraction data (in Å for Cu*K*α) were

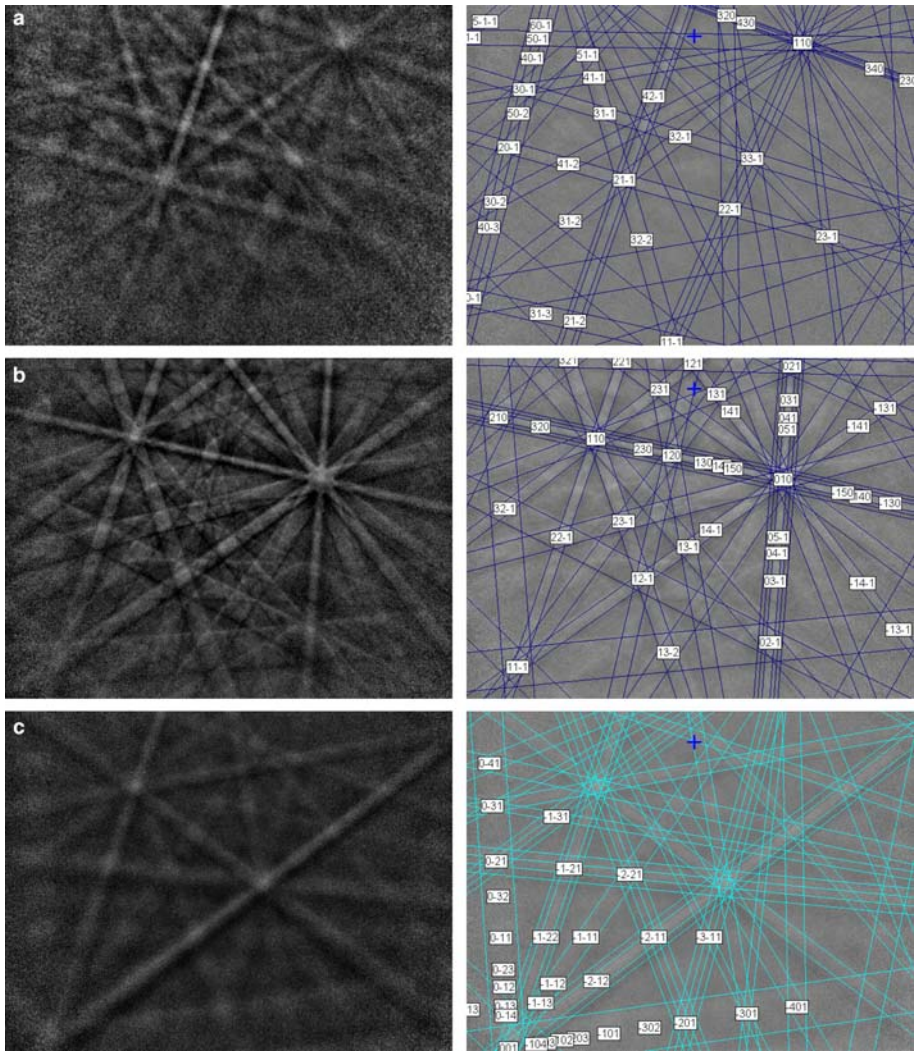

FIG. 6. EBSD patterns obtained at the points shown in Fig. 4*e* by crosses and the fitted result of the EBSD pattern for a working distance of 177 mm: (*a)* dzierżanowskite; (*b*) oldhamite; (*c*) covellite.

calculated from the results of the single-crystal structure refinement of synthetic $CaCu_2S_2$ and are listed in Table 2. The Raman spectrum of dzierżanowskite was recorded at low laser power. At standard power (~44 mW on sample) a crater was burnt in the mineral, and a Ca sulfate spectrum was recorded with a strong S–O stretching band at 1007 cm^{-1} (Fig. 7). Three bands at 300 (Cu–S stretching), 103 and 86 cm^{-1} (Ca–S stretching) are observed in the dzierżanowskite spectrum.

The composition, EBSD pattern and Raman spectrum of dzierżanowskite confirm that it is the natural analogue of synthetic $CaCu_2S_2$ (Purdy, 1998), which belongs to a group of thiocuprates characterized by the formula $[M_a]^{z+}[Cu_bS_c]^{z-}$ (Boller, 2007). These thiocuprates possess a $CaAl_2Si_2$ structure type (Condron *et al.*, 2007). In dzierżanowskite a double tetrahedral layer is formed by CuS_4 edge-linked tetrahedra. There is a layer of Ca octahedra between the layers (Fig. 8*a*). The tetrahedra are arranged one above the other along the *c* axis in such a way that the specific channels containing Ca are visible (Fig. 8*b*).

TABLE 2. Calculated powder X-ray diffraction data for dzierżanowskite ($CuK\alpha_1 = 1.540598$ Å, Debye-Scherrer geometry, no anomalous dispersion, $I_{calc} > 1$).

h	*k*	*l*	d_{calc}	I_{calc}
0	**0**	**1**	**6.523**	**36**
1	**0**	**0**	**3.412**	**28**
0	0	2	3.262	1
1	**0**	**1**	**3.023**	**25**
0	**1**	**1**		**78**
1	**0**	**2**	**2.358**	**100**
0	1	2		5
0	0	3	2.174	14
1	**1**	**0**	**1.970**	**93**
1	1	1	1.886	10
0	**1**	**3**	**1.834**	**22**
1	**0**	**3**		**28**
2	0	0	1.706	3
0	2	1	1.651	3
2	0	1		13
2	**0**	**2**	**1.512**	**1**
0	**2**	**2**		**22**
0	1	4	1.471	3
1	0	4		4
1	**1**	**3**	**1.460**	**22**
0	2	3	1.342	9
2	0	3		7
0	0	5	1.305	2
2	1	0	1.290	3
1	2	1	1.265	9
2	1	1		3
1	0	5	1.219	5
0	1	5		6
2	1	2	1.199	19
1	2	2		1
0	2	4	1.179	2
2	0	4		1
3	0	0	1.137	14
1	2	3	1.109	8
2	1	3		10

The strongest lines are given in bold.

Genesis and growth mechanism of dzierżanowskite

Dzierżanowskite was found in larnite-fluorellestadite-brownmillerite-ye'elimite rocks (Fig. 1, holotype specimen no. MMII-33) and in flamite-fluormayenite-brownmillerite rocks (Fig. 3, specimen no. JBB4), where the primary pyrometamorphic mineral assemblage is similar to the phase content of Portland clinker (Taylor, 1997; Sokol *et al.*, 2014). Larnite (β-Ca_2SiO_4), flamite (α-Ca_2SiO_4), ye'elimite, brownmillerite and mayenite are typical components of clinkers. Flamite is a new mineral, described recently from pyrometamorphic gehlenite hornfelses of the Hatrurim Complex in the Negev Desert, Israel (Sokol *et al.*, 2015; Gfeller *et al.*, 2015*b*).

A distinctive feature of rocks containing dzierżanowskite is the presence of S-bearing minerals of the nabimusaite–dargaite and ternesite–silicocarnotite series (Galuskin *et al.*, 2015*a*, 2016), jasmundite, oldhamite and various sulfides, which are confined to microporous fragments of the rocks. Nabimusaite–dargaite and ternesite–silicocarnotite are products of the high-temperature alteration of primary clinker mineral associations affected by sulfate-halogen-bearing melts (fluids, gases) at temperatures >900°C, which are generated during pyrometamorphism close to the combustion foci (Galuskin *et al.*, 2015*a*,*b*; 2016).

Superimposed melts, fluids, or gases are probably originated as by-products of the combustion of a sedimentary protolith bearing organic fuel and/or combustion of external flows of combustible gases. Under conditions of low lithostatic pressure these gases migrate to the surface along channels and cracks in metamorphosed rocks. Pyrometamorphic gases are heterogeneous and contain not only sulfurous compounds, but also Cl and F, CO_2, water gas and others. These compounds are similar to volcanic gases and to the gaseous products of burning coal seams and waste coal deposits (Mizutani, 1970; Symonds, 1993; Suárez-Ruiz *et al.*, 2012). We have not yet found nitrogen compounds that are typical of burning coals (Suárez-Ruiz *et al.*, 2012). Thus, superimposed mineralogenesis in this case was similar to an ultrahigh-temperature fumarole system.

In the holotype specimen no. MII-33 dzierżanowskite is confined to light, porous fragments of larnite rocks (Fig. 1*a*). Here, recrystallization of clinker minerals and the appearance of high-temperature minerals, nabimusaite–dargaite, jasmundite and diverse sulfides, are notable (Fig. 1*a*, *b*). In specimen no. JBB4 grains of newly-formed jasmundite show sizes up to 1 cm. Jasmundite contains rounded oldhamite inclusions replaced peripherally by Cu-sulfides and also rare micrometre-sized channels (Fig. 3*d*). We consider that jasmundite, which is an S^{2-} bearing phase, is a product of the pneumatolytic (fluid-gaseous) metasomatism of larnite, flamite and fluorellestadite. Oldhamite also formed at that stage from the gas phase as a result of reaction between sulfur-bearing gases (for example, H_2S) and Ca-minerals:

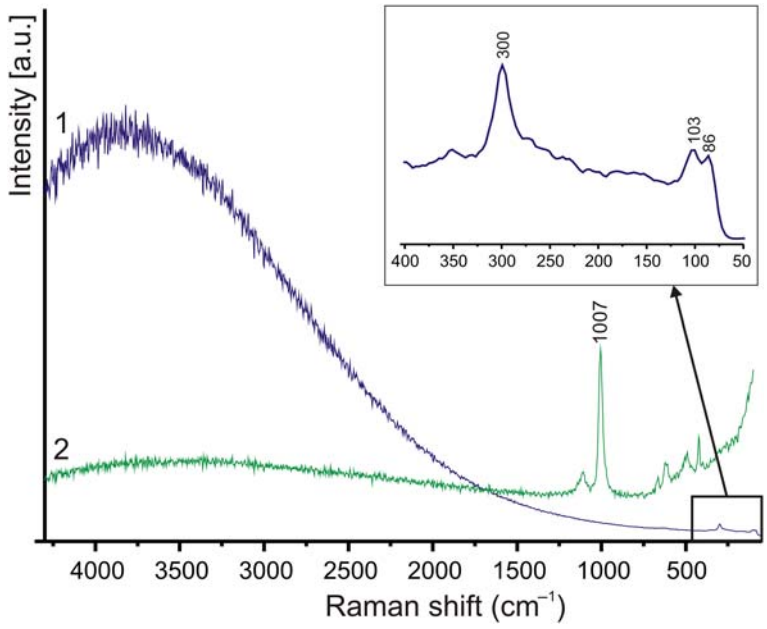

FIG. 7. Raman spectra of dzierżanowskite (1) and products of its alteration, calcium sulfate, formed under the laser beam (2).

$CaO + H_2S = CaS + H_2O$, at temperatures ≈800°C (Westmoreland *et al.*, 1977). The rounded shapes of oldhamite are consistent with the channel cross-section geometry or these are relic forms of Ca-silicate replacement (Fig. 3*d*). At decreasing temperatures to 350–400°C, Cu sulfides formed, for example according to the reaction: $2CuCl + H_2S = Cu_2S + 2HCl$ (Mizutani, 1970). Newly-formed Cu-sulfides were not in equilibrium with previously formed oldhamite, so between them there is a reaction zone of dzierżanowskite formed according to the reaction: $Cu_2S + CaS = CaCu_2S_2$. The same reaction was used for formation of the synthetic analogue of dzierżanowskite, which is

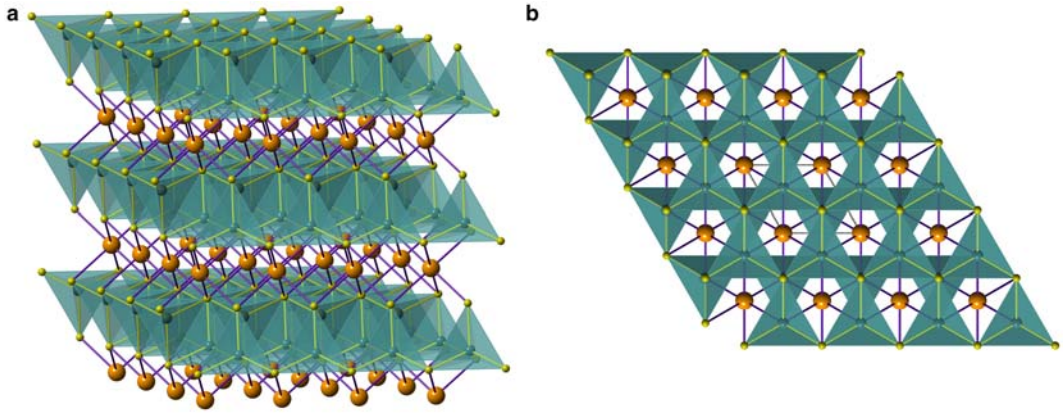

FIG 8. (*a*) The dzierżanowskite structure ($CaAl_2Si_2$ structure type) formed by two tetrahedral layers (CuS_4), where tetrahedra are linked by edges. Calcium ions with octahedral coordination are arranged between tetrahedral layers. (*b*) The packing mode of tetrahedral layers defines channels along the *c* axis, where calcium is located. Cu – green-blue balls, Ca – orange balls, S – yellow balls.

synthesized at temperatures ≈400°C (Purdy, 1998). Dzierżanowskite is preserved only as inclusions in jasmundite, and more rarely inside other silicates. Fluormayenite associated with dzierżanowskite was replaced by fluorkyuygenite by the reaction $Ca_{12}Al_{14}O_{32}[\square_4F_2] + 4H_2O = Ca_{12}Al_{14}O_{32}[(H_2O)_4F_2]$, as a result of overheated water vapour action. Fluorkyuygenite defects in the fluormayenite structure are stable at temperatures below 400°C (Galuskin *et al.*, 2015*b*). Cuprite and malachite developed after dzierżanowskite in the fluorkyuygenite bearing zone. Dzierżanowskite, along with nabimusaite, gazeevite, silicocarnotite and fluorkyuygenite in the pyrometamorphic rocks of the Hatrurim Complex, testifies to a superimposed new stage of the high-temperature alteration of pyrometamorphic rocks (natural clinker of the sanidinite facies). Such alteration was determined by by-products (melts/fluids and gases) of pyrometamorphism which originated in the deeper levels of combustion (Galuskina *et al.*, 2014; Galuskin *et al.*, 2015*a*,*b*, 2016).

Acknowledgements

The authors thank Prof. Raymond MacDonald (University of Warsaw) for English correction. The authors thank reviewers (R. Miyawaki and I.V. Pekov) for their useful and constructive comments. The work was supported by the National Science Centre (NCN) of Poland, grant no. UMO-2013/11/B/ST10/00272.

References

Bentor, Y.K. (editor) (1960) Israel. In: *Lexique Stratigraphique International, Asie*, Vol. III, (10.2). Centre national de la recherche scientifique, Paris.

Boller, H. (2007) Thiocuprates – interesting anisotropic solids. *Journal of Alloys and Compounds*, **442**, 3–10.

Burg, A., Starinsky, A., Bartov, Y. and Kolodny, Y. (1991) Geology of the Hatrurim Formation ("Mottled Zone") in the Hatrurim basin. *Israel Journal of Earth Sciences*, **40**, 107–124.

Burg, A., Kolodny, Y. and Lyakhovsky, V. (1999) Hatrurim-2000: The "Mottled Zone" revisited, forty years later. *Israel Journal of Earth Sciences*, **48**, 209–223.

Condron, C.L., Hope, H., Piccoli, P.M.B., Schultz, A.J. and Kauzlarich, S.M. (2007) Synthesis, structure, and properties of $BaAl_2Si_2$. *Inorganic Chemistry*, **46**, 4523–4529.

Day, A. and Trimby, P. (2004) *Channel 5 Manual*. HKL Technology Inc., Hobro, Denmark.

Galuskin, E., Galuskina, I., Kusz, J., Armbruster, T., Marzec, K., Dzierżanowski, P. and Murashko, M. (2014) Vapnikite Ca_3UO_6 – a new double perovskite mineral from pyrometamorphic larnite rocks of the Jabel Harmun, Palestine Autonomy, Israel. *Mineralogical Magazine*, **78**, 571–581.

Galuskin, E.V., Gfeller, F., Armbruster, T., Galuskina, I.O., Vapnik, Y., Murashko, M., Włodyka, R. and Dzierżanowski, P. (2015*a*) New minerals with a modular structure derived from hatrurite from the pyrometamorphic Hatrurim Complex. Part I. Nabimusaite, $KCa_{12}(SiO_4)_4(SO_4)_2O_2F$, from larnite rocks of Jabel Harmun, Palestinian Autonomy, Israel. *Mineralogical Magazine*, **79**, 1061–1072.

Galuskin, E.V., Gfeller, F., Armbruster, T., Sharygin, V.V., Galuskina, I.O., Krivovichev, S.V., Vapnik, Y., Murashko, M., Dzierżanowski, P. and Wirth, R. (2015*b*) Mayenite supergroup, part III: Fluormayenite, $Ca_{12}Al_{14}O_{32}[\square_4F_2]$, and fluorkyuygenite, $Ca_{12}Al_{14}O_{32}[(H_2O)_4F_2]$, two new minerals from pyrometamorphic rocks of the Hatrurim Complex, South Levant. *European Journal of Mineralogy*, **27**, 123–136.

Galuskin, E.V., Galuskina, I.O., Gfeller, F., Krüger, B., Kusz, J., Vapnik, Y., Dulski, M. and Dzierżanowski, P. (2016) Silicocarnotite, $Ca_5[(SiO_4)(PO_4)](PO_4)$, a new 'old' mineral from the Negev Desert, Israel, and the ternesite-silicocarnotite solid solution: indicators of high-temperature alteration of pyrometamorphic rocks of the Hatrurim Complex, Southern Levant. *European Journal of Mineralogy*, **28**, 105–12.

Galuskin, E.V., Gfeller, F., Galuskina, I.O., Armbruster, T., Krzątała, A., Vapnik, Ye., Kusz, J., Dulski, M., Gardocki, M., Gurbanov, A.G. and Dzierżanowski, P. (2017) New minerals with modular structure derived from hatrurite from the pyrometamorphic rocks, Part III: Gazeevite, $BaCa_6(SiO_4)_2(SO_4)_2O$, from Israel and Palestine Autonomy, South Levant and from South Ossetia, Greater Caucasus. *Mineralogical Magazine*, **81**, 499–513.

Galuskina, I.O., Vapnik, Y., Lazic, B., Armbruster, T., Murashko, M. and Galuskin, E. (2014) Harmunite $CaFe_2O_4$: A new mineral from the Jabel Harmun, West Bank, Palestinian Autonomy, Israel. *American Mineralogist*, **99**, 965–975.

Gfeller, F., Galuskina, I.O., Galuskin, E.V., Armbruster, T., Vapnik, Y., Dulski, M., Gardocki, M., Jeżak, L. and Murashko, M. (2015*a*) Dargaite, IMA2015-068. CNMNC Newsletter No. 28, December 2015, page 1860; *Mineralogical Magazine*, **79**, 1859–1864.

Gfeller, F., Widmer, R., Krüger, B., Galuskin, E.V., Galuskina, I.O. and Armbruster, T. (2015*b*) The crystal structure of flamite and its relation to Ca_2SiO_4 polymorphs and nagelschmidtite. *European Journal of Mineralogy*, **27**, 755–769.

Gross, S. (1977) The mineralogy of the Hatrurim Formation, Israel. *Geological Survey of Israel Bulletin*, **70**.

Kachalovskaya, V.M., Osipov, B.S., Nazarenko, N.G., Kukoev, V.A., Mazmanyan, A.O., Egorov, I.N. and Kaplunnik, L.N. (1988) Chvilevaite – a new alkali sulfide with the composition $Na(Cu,Fe,Zn)_2S_2$. *Zapiski VMO*, **117**(2), 204–207.

Kaplunnik, L.N., Petrova, I.V., Pobedimskaya, E.A., Kachalovskaya, V.M. and Osipov, B.S. (1990) Crystal structure of natural alkaline sulfide chvilevaite $Na(Cu,Fe,Zn)_2S_2$. *Soviet Physics Doklady*, **35**, 6–8.

Kolodny, Y. and Gross, S. (1974) Thermal metamorphism by combustion of organic matter: isotope and petrological evidences. *Journal of Geology*, **82**, 489–506.

Mizutani, Y. (1970) Copper and zinc in fumarolic gases of Showashinzan volcano, Hokkaido, Japan. *Geochemical Journal*, **4**, 87–91.

Novikov, I., Vapnik, Y. and Safonova, I. (2013) Mud volcano origin of the Mottled Zone, South Levant. *Geoscience Frontiers*, **4**, 597–619.

Picard, L. (1931) *Geological Research in the Judean Desert*. Goldberg Press, Jerusalem.

Purdy, A.P. (1998) Ammonothermal crystal growth of sulfide materials. *Chemistry of Materials*, **10**, 692–694.

Sokol, E.V., Novikov, I.S., Vapnik, Y. and Sharygin, V.V. (2007) Gas fire from mud volcanoes as a trigger for the appearance of high-temperature pyrometamorphic rocks of the Hatrurim Formation (Dead Sea area). *Doklady Earth Sciences*, **413A**, 474–480.

Sokol, E., Novikov, I., Zateeva, S., Vapnik, Y., Shagam, R. and Kozmenko, O. (2010) Combustion metamorphism in the Nabi Musa dome: new implications for a mud volcanic origin of the Mottled Zone, Dead Sea area. *Basin Research*, **22**, 414–438.

Sokol, E.V., Kokh, S.N., Vapnik, Y., Thiéry, V. and Korzhova, S.A. (2014) Natural analogs of belite sulfoaluminate cement clinkers from Negev Desert, Israel. *American Mineralogist*, **99**, 1471–1487.

Sokol, E.V., Seryotkin, Y.V., Kokh, S.N., Vapnik, Y., Nigmatulina, E.N., Goryainov, S.V., Belogub, E.V. and Sharygin, V.V. (2015) Flamite, $(Ca,Na,K)_2(Si,P)O_4$, a new mineral from ultrahigh-temperature combustion metamorphic rocks, Hatrurim Basin, Negev Desert, Israel. *Mineralogical Magazine*, **79**, 583–596.

Suárez-Ruiz, I., Flores, D., Filho, J.G.M. and Hackley, P. C. (2012) Review and update of the applications of organic petrology: Part 2, geological and multidisciplinary applications. *International Journal of Coal Geology*, **98**, 73–94.

Symonds, R. (1993) Scanning electron microscope observation of sublimates from Merapi volcano, Indonesia. *Geochemical Journal*, **26**, 337–350.

Taylor, H.F.W (1997) *Cement Chemistry.* Thomas Telford Publishing, London.

Vapnik, Y., Sharygin, V.V., Sokol, E.V. and Shagam, R. (2007) Paralavas in a combustion metamorphic complex: Hatrurim Basin, Israel. *Reviews in Engineering Geology*, **18**, 1–21.

Westmoreland, P.R., Gibson, J.B. and Harrison, D.P. (1977) Comparative kinetics of high-temperature reaction between H_2S and selected metal oxides. *Environmental Science and Technology*, **11**, 488–491.